Research Article
Open Access

Life Sciences, Medicine and Biomedicine

Nano-cockle shell powder and alginate as novel injectable bone filler: A preliminary formulation and characterization study

Penny George[1], Zariyantey Abdul Hamid[1], Md Zuki Abu Bakar[2] and B Hemabarathy Bharatham[1,3*]

[1]Biomedical Science Programme, School of Health and Applied Sciences, Faculty of Health Sciences, Universiti Kebangsaan Malaysia, Jalan Raja Muda Abdul Aziz, 50300 Kuala Lumpur, Malaysia.
[2]Department of Veterinary Preclinical Sciences, Faculty of Veterinary Medicine, Universiti Putra Malaysia, Persiaran, UPM, Mardi, 43400 Serdang, Selangor Darul Ehsan, Malaysia.
[3]Curtin Medical School, Faculty of Health Sciences, Curtin University, Bentley, Western Australia 6102, Australia.

***Correspondence:** hema.bharatham@curtin.edu.au

Received: 29 September 2023; **Revised:** 5 April 2024; **Accepted:** 9 April 2024; **Published:** 31 May 2024
DOI https://doi.org/10.28916/lsmb.8.1.2024.138

ABSTRACT

Cockle shells of the *Anadara granosa* species consist of 95-99% aragonite form of calcium carbonate ($CaCO_3$) crystals. Aragonites are known to be denser which allows it to be incorporated, resolved and replaced by bone tissues over time when used in bone tissue grafting. An injectable biomaterial-based bone filler with appropriate injectability and biological properties was formulated using powdered cockle shells in nanoscale (nCSP) and sodium alginate (Alg). Initial attempts in formulating the bone filler using alginate and citric acid as a setting agent in the composition of nCSP: Alg of 60: 40, 70: 30 and 80: 20 wt.% produced variable results in the bone filler characterization. Characterization study of nCSP-Alg bone filler with 70:30 wt.% compositions showed excellent injectability ($p<0.05$), viscosity ($p<0.05$) and anti-washout ability that was further evaluated through physicochemical analysis, morphology and biocompatibility studies. Scanning electron micrographs revealed plate-like nanocrystal deposits with micropores ranging between 1.5 – 7.4 µm. XRD and FTIR evaluation indicated the presences of peaks associated with aragonite form of $CaCO_3$. Biocompatibility studies with MG63 osteoblast showed osteoconductivity of the bone fillers with excellent cell adherence, growth and subsequent mineralization of the matrices. In conclusion, nCSP-Alg biomaterial-based bone filler with 70:30 wt.% compositions shows promising use as a cost effective bone grafting material for clinical application in the field of bone tissue engineering.

Keywords: *Cockle shell; sodium alginate; bone filler and MG63 osteoblast*

INTRODUCTION

In the past decades, the use of biomaterials has seen an exponential growth in the range of materials available for bone tissue engineering that can be tailored in regard to compositions, architecture, compatibility and degradability. The new generation of bone substitute materials such as the bioactive bone cements that are mouldable with self-setting properties are highly sort after as bone fillers, graft extenders as well as implant stabilizers. Despite the low

mechanical strength limiting their use in loadbearing areas, these bioactive materials with osteoconductive properties are highly useful as bone fillers (Sony et al., 2015). An injectable bone filler reduces the need for surgical invasion and provides easy delivery to sites of limited accessibility making these materials to be in high demands for minor bone defect repairs and gap bridges. Biomimetic fabrication strategies become a great point to look at, where the structure is highly controlled and optimized at several length scales. These materials must be biocompatible and biodegradable to provide an optimum function for tissue regeneration.

Calcium carbonate nanoparticles are inorganic biomaterials with various morphological structures that have attracted the interest of researchers from various fields. This interest is due to the wide application properties of these nanoparticles such as in paint, rubber, and plastics industries. With the present focus of interest in nanotechnology, calcium carbonate nanoparticles have been shown to be biocompatible for use in medicine, pharmaceutical industries as well as for drug delivery systems (Fukui & Fujimoto, 2012).

Shells from Mollusca family such as cockle shells are one of the major sources of calcium carbonate. Cockle shells consist approximately 98-99% calcium carbonate as the primary component (Mohamed et al., 2012, Bharatham et al., 2014). As shown in previous studies, the cockle shell powder consists of an aragonite form of calcium carbonate which could be manipulated in correct formulation to produce materials with higher strength and efficacy yet displaying good injectability properties. Interestingly, aragonite calcium carbonate is known to be biocompatible with better potentials to be naturally converted to bone.

The use of polymers in the formulation of a bone scaffold is highly required to produce a stable material with a reduced degradation property that ensures early-stage material lost is prevented. Polymers both natural and synthetic provides a wide range of choice for researchers in the quest of material fabrication. One such naturally occurring polymer is the alginate. This polysaccharide has been widely studied in tissue engineering and drug delivery system due to its gelation and cross-linking properties that can be modified to produce some desired features such as stability and porosity (Venkatesan et al., 2014).

Understanding the characteristics of the bone filler material regarding material physiochemical properties and surface architecture upon setting is vital to determine the success of cellular growth and integration. The interaction of osteoblast towards the filler material and evaluation of the stages of cellular attachment, proliferation and growth will enable us to understand the biocompatibility and duration that is required for tissue regeneration. This study is carried out using nano cockle shell powder and alginate as the main composition mixture, that are modified to form an injectable biomaterial-based filler material for bone tissue application that are further evaluated for its injectability, rheological properties, phase reaction, microstructure and biocompatibility.

METHODOLOGY

Fabrication of bone filler

Fabrication of the bone filler is conducted using nano cockle shell powder (nCSP) which was prepared according to a previously reported method (Mahmood et al., 2017). The prepared nCP are pre-weighed prior to being combined with deionized water liquefied alginate solution (Alg) that was homogenized at 700 rpm to obtain a smooth slurry in different ratio. The fabrication of the biomaterial filler is done based on modified method (Alves et al., 2010) in three different compositions of nCSP: Alg of 60:40, 70:30 and 80:20 wt%. 0.02 ml liquid citric acid is then added as a setting agent until a workable consistency is formed. The prepared fillers were loaded into a syringe prior to be used for characterization studies.

Initial characterization study

Injectability

Injectability studies were conducted according to the methods reported by Maulida (Maulida et al., 2015). Prepared sample mixtures are quickly loaded into a 10 ml syringe, and a 5-kg compressive load was mounted vertically on the top of the plunger for 2 minutes. The initial and final mass of the samples were measured, and the injectability was calculated according to the following equation:

$$Injectability\ (\%) = \frac{Mass\ expelled\ from\ the\ syringe}{Total\ mass\ of\ the\ sample\ before\ injecting}\ x\ 100\%$$

Viscosity

The viscosity of the filler material was measured according to the method described by Sato (Sato et al., 2017). Prepared sample mixture was loaded into a cylindrical shaped mould with a 5 mm diameter and 5 mm height. The moulded samples were then placed on a glass plate and compressed using a 2 kg glass plate for 10 minutes. Area of dispersion of sample materials were measured using a digital photograph with the ImageJ software.

Anti-washout study

The anti-washout ability test was conducted in accordance with the method described by Lin (Lin et al., 2010) with some modification. Prepared samples were loaded into a mould with a 2 mm diameter and 2 mm height. The moulded samples were then immediately soaked in 50 ml simulated body fluid (SBF, pH 7.40) placed on 90 rpm 37°C shaker for 12 hours. Semi quantitative scoring was used to evaluate the anti-washout ability according to the criteria in Table 1.

Table 1

Criteria for semi quantitative scoring

Criteria	Score
Stable bone filler without visible disintegration	0
Bone filler with damaged surface	1
Bone filler with partial disintegration	2
Disintegration of the whole structure of the bone filler	3

Physiochemical, morphology and biocompatibility studies

X-Ray Diffraction (XRD) analysis

Crystallinity of the compound found in the bone filler is analysed using X-ray powder diffractometer (XRD) (Shimadzu XRD-6000, Japan powder diffractometer) with CuKα (λ=1.540562 Å) at 40 kV and 30 mA using 1–2 g of ground sample of pre-set harden filler material. Scanning rate used to produce the diffraction form was 0.02 degrees per second in 2θ at a range of 20° to 80°.

Fourier Transform Infrared (FTIR) analysis

FTIR analysis is carried out to identify the chemical functionality of the bone filler using Agilent technologies, Cary 630 FTIR spectrophotometer, over the range of 4000 cm^{-1} to 650 cm^{-1}. 0.1 mg of samples were prepared and spectra were taken at 8 cm^{-1} resolution and 4 cm^{-1} scans.

Morphology studies

Prepared samples of nCSP-Alg bone filler were allowed to set prior to be placed on a stub and sputter coated with gold for scanning electron microscope (SEM) observations. The average pore diameter of the bone filler was calculated based on 30 measurements measured from various angles on the micrograph image. SEM observations were also conducted on 24 hours SBF immersed bone filler samples for observational studies on apatite formation.

Osteoblast morphology changes

Morphological changes of MG-63 human osteoblast seeded on to the fabricated bone fillers moulded into a cylindrical scaffold were observed at days 3, 7 and 14 using scanning electron microscopy. Sterile cylindrical bone scaffolds (5 mm diameter and 5 mm height) were seeded with 100 000 cells/100 µl/scaffold in a 6 well culture plate. At the end of the designated time period, culture medium was removed and the scaffolds were fixed with 2.5% glutaraldehyde solution and processed according to standard protocols of scanning electron microscope sample preparation

Statistical analysis

All quantitative data were analysed using one-way analysis of variance (ANOVA). The results were shown as mean ± standard error (SE). Post hoc test were done for statistically significant values $p<0.05$ using Tukey's Multiple Comparison Test. All descriptive and inferential statistical analyses were performed using Excel version 2010 and SPSS version 21.0.

RESULTS

Bone filler initial characterization studies

Injectability and viscosity

Percentage of injectability of the bone filler according to different formulations are shown in Figure 1. Percentage of injectability for nCSP-Alg bone filler with 80:20 wt.% composition (84.7 ± 0.99%) was significantly higher ($p<0.05$) compared to nCSP-Alg bone filler with 70:30 wt.% (46.1 ± 4.77%) and 60:40 wt.% (20.79 ± 3.17%) compositions.

Figure 1

Percentage of injectability

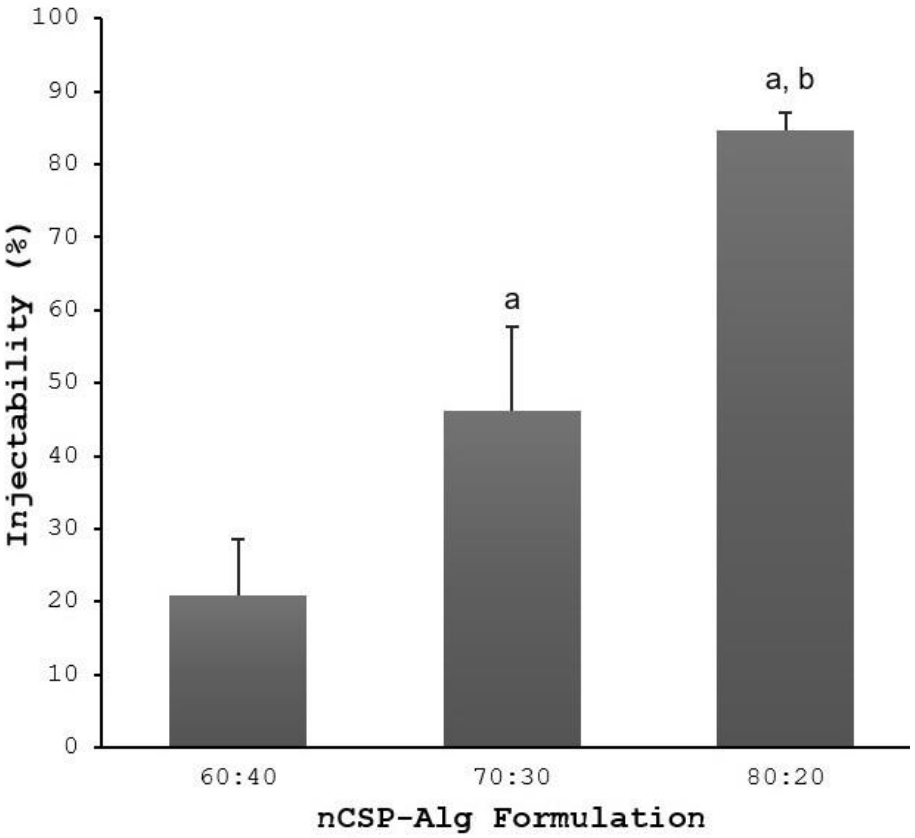

Note: Percentage of injectability according to the formulation of nCSP-Alg bone filler. [a] significant difference compared to 60:40 wt.% composition. [b] significant difference compared to 70:30 wt.% composition.

Result in Figure 2 shows the viscosity of the bone fillers. The results showed that nCSP-Alg bone filler with 80:20 wt.% composition (942.87 ± 12.08 mm^2) had the most widely dispersed area compared to nCSP-Alg bone filler with 70:30 wt.% (804.38 ± 21.62 mm^2) and 60:40 wt.% (733.74 ± 22.84 mm^2) and the difference was significant at $p<0.05$.

Figure 2

Viscosity of the bone fillers

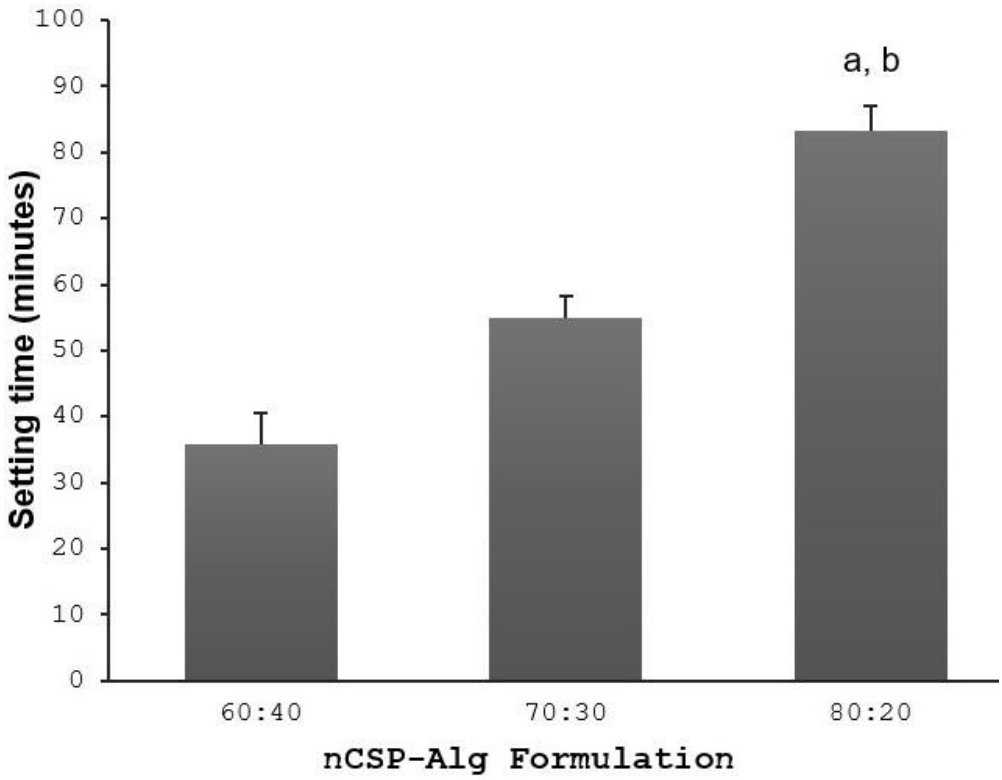

Note: Spread area according to the formulation of nCSP-Alg bone filler. [a] significant difference compared to 70:30 wt.% composition. [b]significant difference compared to 60:40 wt.% composition.

Anti-washout study

Semi quantitative scoring for the anti-washout ability of the bone filler was conducted based on the criteria described earlier (Table 1). Table 2 shows the score of the anti-washout ability of the bone fillers from the semi-quantitative study and the corresponding images of the bone fillers before and after immersion in SBF for 12 hours. The nCSP-Alg bone filler with 60:40 wt.% and 70:30 wt.% compositions showed stable characteristics with a score of '0' which indicate that the fabricated bone fillers were stable without disintegration as supported by its corresponding figures. The score increased for nCSP-Alg bone filler with 80:20 wt.% composition (score 2) where partial breakdown of the bone filler was observed.

Table 2

Anti-washout study

nCSP-Alg composition	Average score (n=6)	Before	After
60:40	0	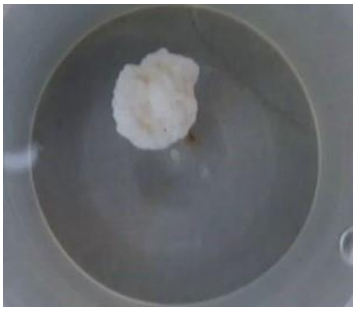	
70:30	0	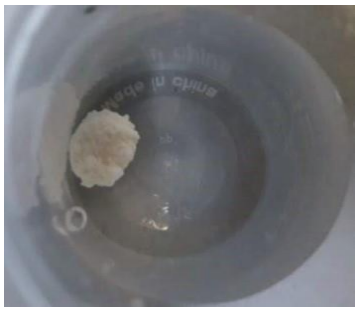	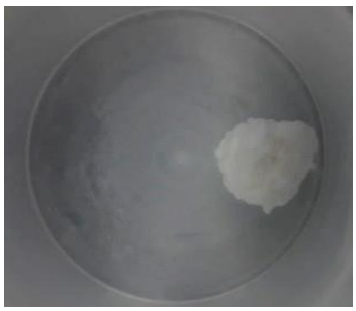
80:20	2		

Note: Semi-quantitive score for anti-washout study and images of nCSP-Alg bone fillers before and after immersing in SBF for 12 hours.

Physiochemical, morphology and biocompatibility

Based on the initial characterization studies, nCSP-Alg bone filler with 70:30 wt.% composition was found to exhibit the best properties of injectability, viscosity and anti-washout ability thus was further analysed for physiochemical, morphology and biocompatibility.

X-Ray Diffraction (XRD) analysis

Figure 3 shows the XRD pattern for alginate(a), nCSP(b) and the nCSP-Alg bone filler (c) with 70:30 wt.% composition. The XRD pattern obtained for nCSP-Alg bone filler corresponds to the features of the aragonite phase peak (file number: PDF 00-024-0025 $CaCO_3$ Aragonite) as noted from the diffractogram.

Figure 3

XRD Diffractogram

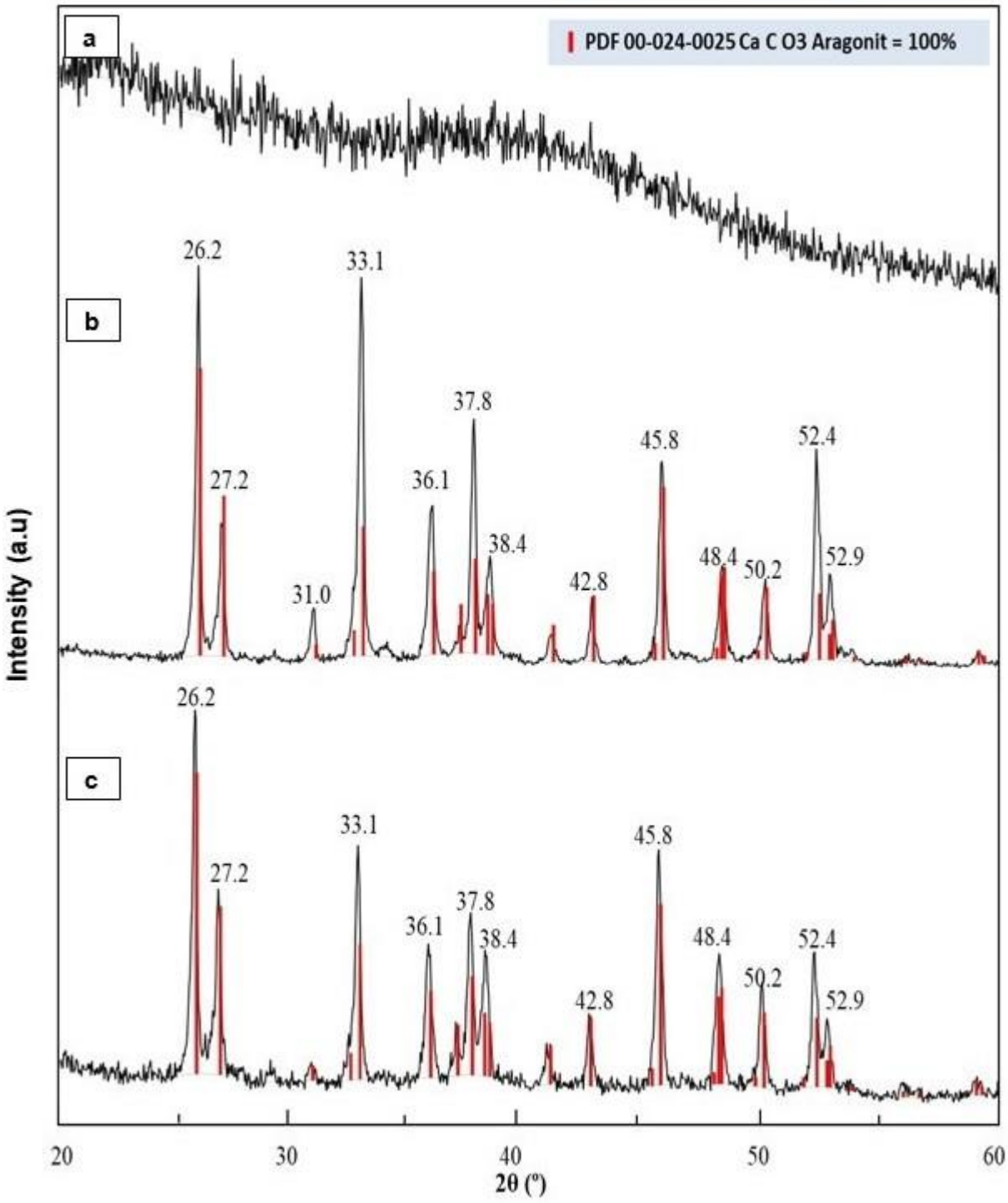

Note: XRD Diffractogram Alg (a), nCSP (b) and nCSP-Alg bone filler with 70:30 wt.% composition(c).

Fourier Transform Infrared (FTIR) analysis

FTIR spectra of nCSP(a), sodium alginate (b) and nCSP-Alg (c) are shown in Figure 4. This spectrum consists of a range of bands between 4000 cm^{-1} to 600 cm^{-1}. Most peaks for nCSP and nCSP-Alg bone filler with 70:30 wt.% composition was found to be matched with each other. The carbonate absorption peaks (1450, 1080, 857, and 707 cm^{-1}) were very apparent in the FTIR pattern of nCSP-Alg bone filler as shown in Figure 4(c).

Figure 4

FTIR spectra

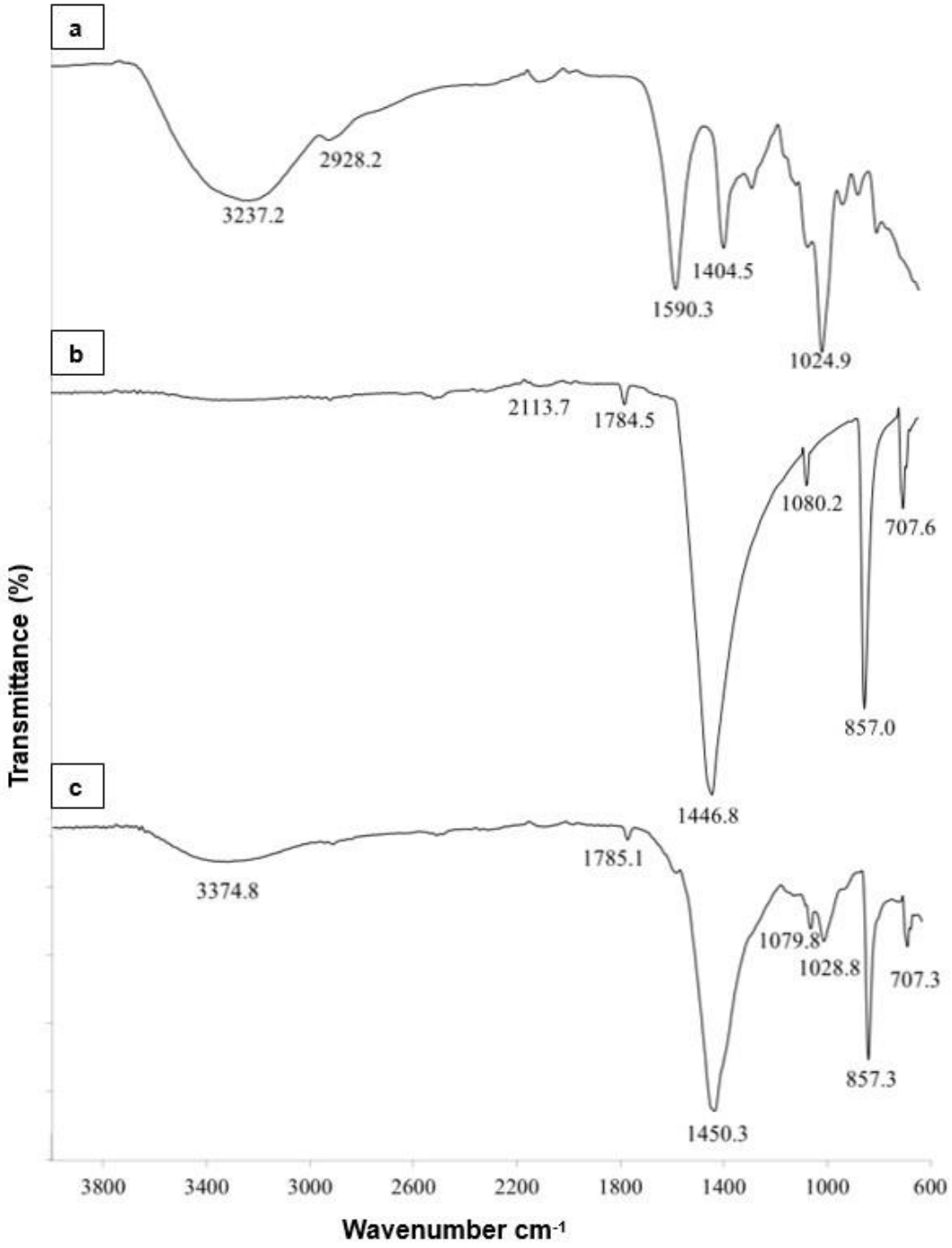

Note: FTIR spectra of Alg (a), nCSP (b) and nCSP-Alg bone filler with 70:30 wt.% composition (c).

Bone filler morphology study

The SEM micrograph for bone filler nCSP-Alg 70:30 wt.% at different levels of magnification (Figure 5) shows the surface morphology in regard to the surface texture, porosity, size and diameter of the pores formed. The presence of micropores within the diameter range of 1.5-7.4μm and formation of plate-like nanocrystal deposits forming agglomerated can be observed in Figure 5(b). The presence of rod-like nCSP crystallites deposition is shown by the red arrows in Figure 5(c).

Figure 5

SEM micrographs of nCSP-Alg 70:30 wt.% surface morphology

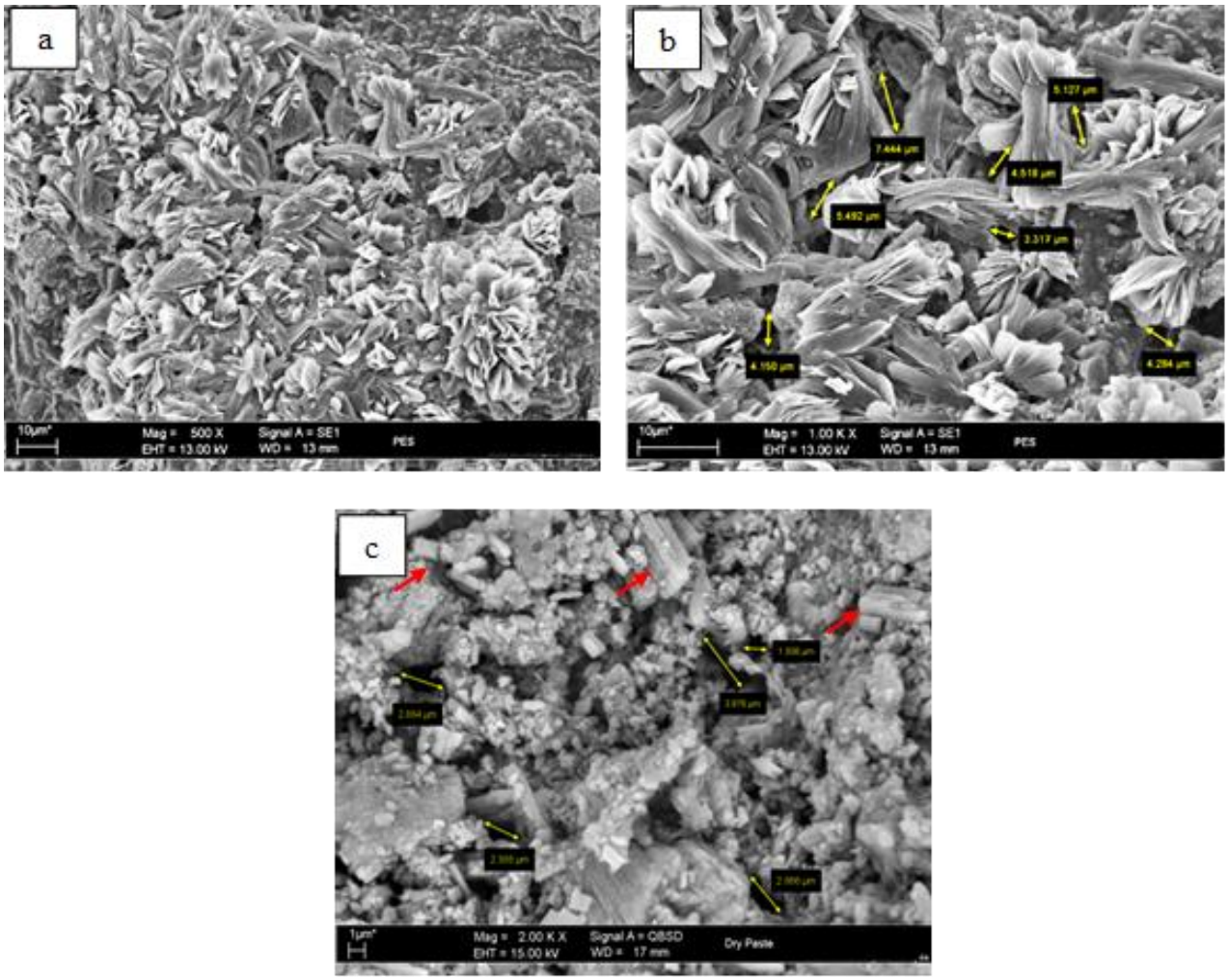

Note: Micrographs of bone filler nCSP-Alg 70:30 wt.% at magnification of x500 (a), x1000 (b) and x2000 (c). Red arrows represent the deposition of nCSP crystallite.

SEM micrograph in Figure 6a, b and c shows the surface morphological changes of the bone filler upon 24 hours immersion in SBF. The presence of polymer fiber network (Figure 6c) depicts the ability of the bone filler to mineralize when in contact with human body fluid.

Figure 6

SEM micrographs of bone filler nCSP-Alg 70:30 wt.% after mineralization study

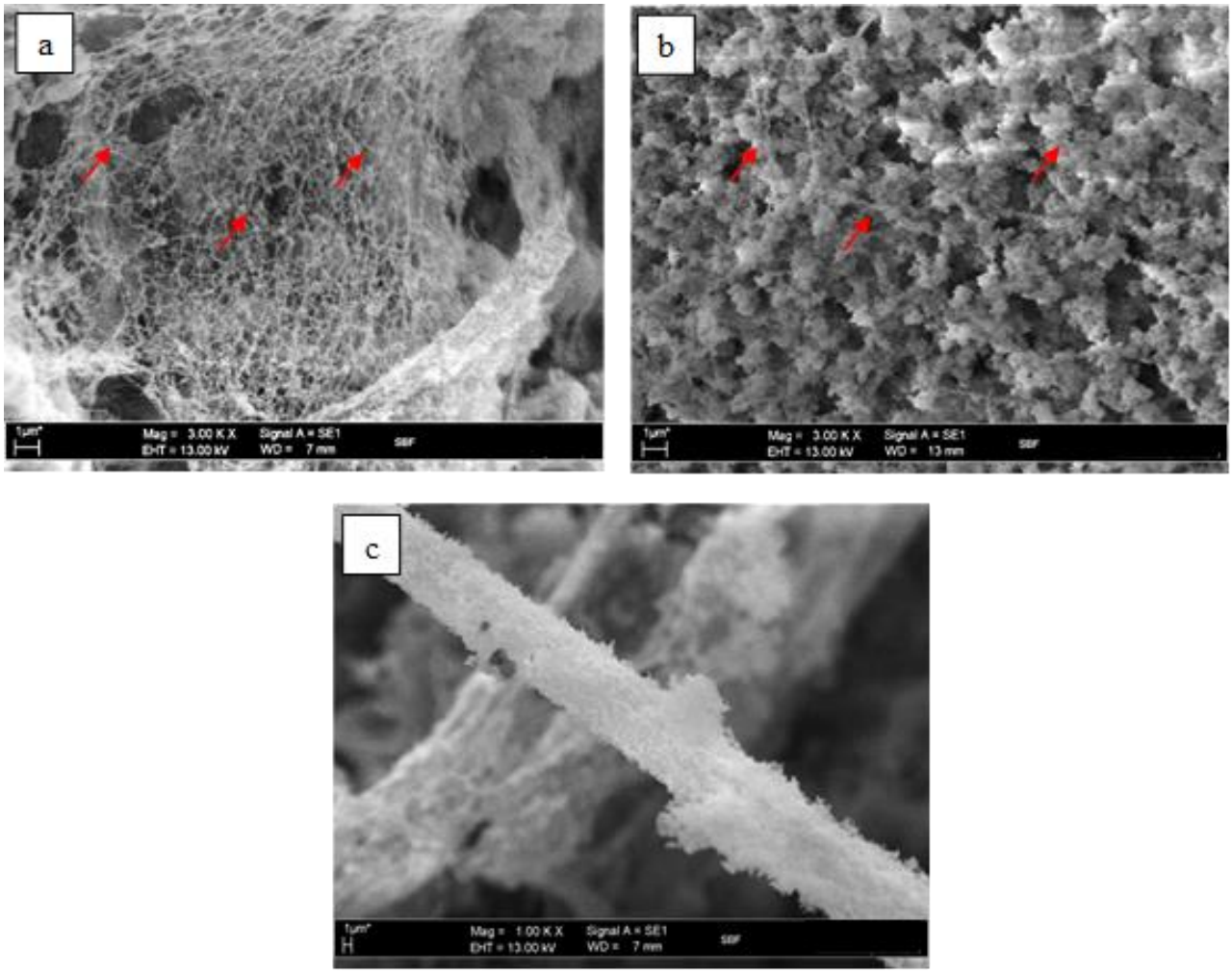

Note: Micrographs of bone filler nCSP-Alg 70:30 wt.% after mineralization study which shows apatite layer formation (arrows) at the magnification of x3000 (a and b) and presence of network fibre at x1000 (c).

Osteoblast morphology changes

Figure 7 (a-i) shows the SEM image of osteoblast cultured on a pre-set bone filler scaffold at days 3, 7 and 14. Day 3 observation showed excellent adherence of the cells on the surface of the scaffolds and cells were generally round in shape (Figure 7a – 7c) with evidence of cytoplasmic extensions. Morphological changes of cell structure were evident by day 7 onwards (Figure 7d-7f) as the cells flattens to envelope the scaffolds. At this stage polygonal cells, filopodia and lamellipodia extension became obvious contributing to a generally roughened surface area. By day 14 surface morphology of the scaffolds shows evidence of complete matrix mineralisation (Figure 7g-7i) with presence of calcium nodules on varying sizes (yellow arrow).

Figure 7

SEM micrographs of bone filler cultured with MG-63 osteoblast.

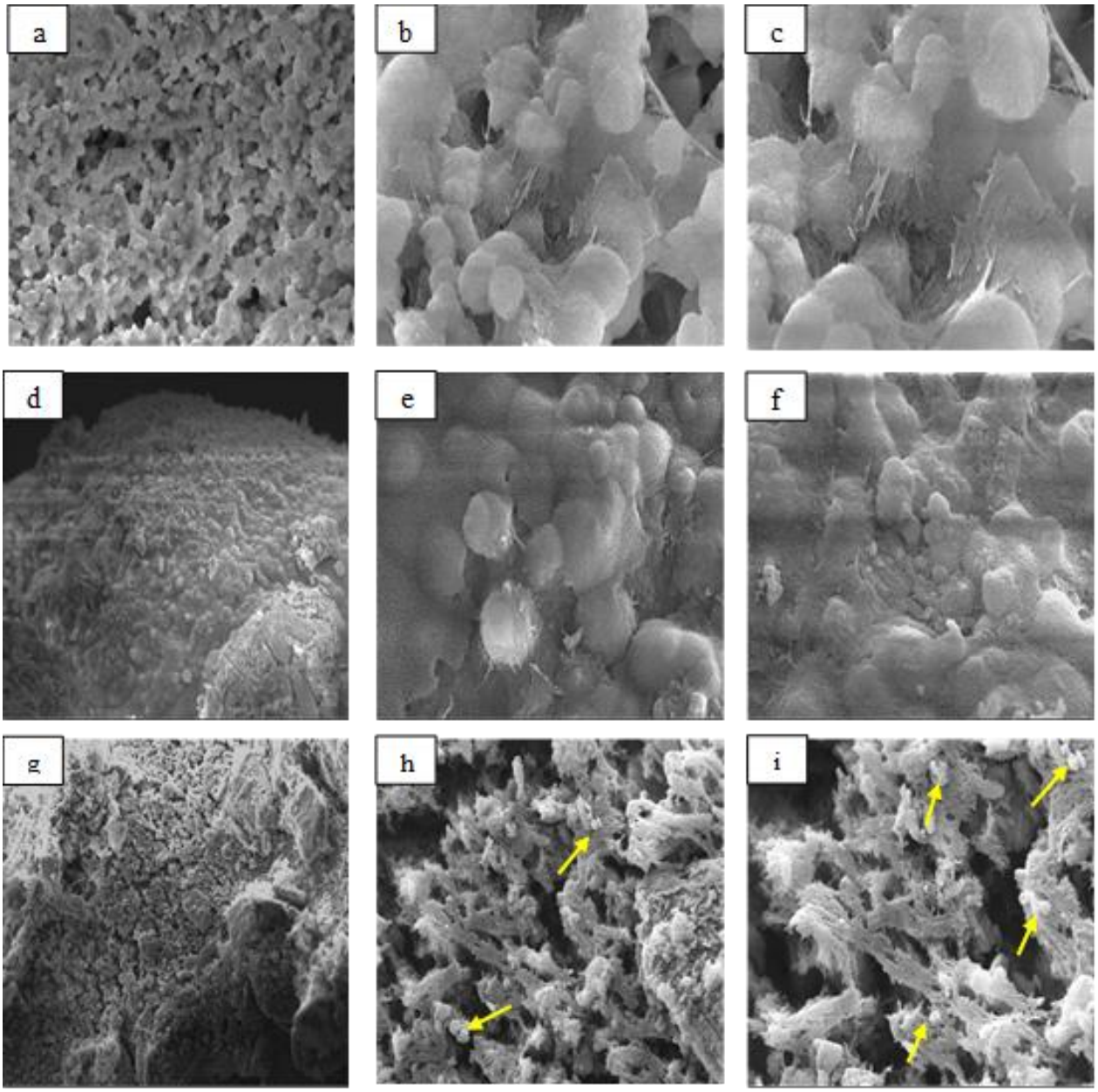

Note: Micrograph of bone filler cultured with MG-63 osteoblast on day 3 at (a) x500, (b) x3000, (c) x5000; day 7 at (d) x500, (e) x3000, (f) x5000 and day 14 at (g) x500, (h) x3000, (i) x5000. Arrows indicate calcium nodule depositions.

DISCUSSION

Bone graft related surgeries contributed to over four million operations worldwide making it the second most common transplantation procedure performed (Turnbull et al., 2018). The field of bone tissue engineering is constantly expanding due to the high demand of bone grafting materials and the constant search for developing bioactive three-dimensional grafts capable of supporting bone regeneration. Mimicking the actual tissue composition would allow greater biological applicability that hence has become a major goal of bone tissue engineering (Ortiz et al., 2017). An ideal grafting material is expected to promote mineralization and osteoid tissue deposition to aid the regeneration process of the bone, thus generating new functional tissues. The fabrication of bone scaffolds using nano cockle shell-alginate were first attempted in 2014 (Bharatham et al., 2014) in the form of a three-dimensional scaffold. In this study, similar combination of material was used to fabricate an injectable formulation to be used as bone fillers. The fabrication attempt was carried out by varying the ratio of nano cockle shell powder (nCSP) and alginate (Alg) (nCSP: Alg wt%) as 80:20, 70:30 and 60:40. A homogenous paste was able to be formed by using 0.02ml of citric acid that acts as a setting agent in the formulation. The final compositions were then subjected to characterization studies which included injectability, viscosity and anti-washout ability.

Characterization studies on injectability and viscosity showed that the increase in the concentration of alginate significantly reduced these characteristics of the bone filler. Alginate is a non-toxic water-soluble polysaccharide (Burguera et al., 2011, Carey et al., 2005) and is often used as a gelling agent. Due to its ability to form hydrogen bonds with water, it increases the cohesiveness of the bone filler, making it more difficult for the solid phase to be separated from the liquid phase. The combination of a higher concentration of alginate with nCSP eventually reduces the injectability and viscosity. When the concentration of alginate is lowered to 20% in the 80:20 wt% combination, a higher injectability and viscosity rate was evident. In contrast the nCSP-Alg bone filler with 60:40 wt.% exhibited the weakest properties of injectability and viscosity due to the higher content of alginate. Injectability characteristic is often emphasized as it plays a substantial role in clinical application involving defects or damages due to limited access (Bohner & Baroud, 2005).

The important effects of alginate in the formulation are also noted through the anti-washout study. Both bone fillers with 60:40 wt.% and 70:30 wt.% compositions maintained their original structure without disintegration compared to 80:20 wt.% composition which showed surface erosion with a higher structural disintegration. Addition of sodium alginate in the formulation of a paste has been previously showed to produce a water-insoluble effect thus reducing the penetration of fluid into the material and increasing its resistance to washout (Lin et al., 2010). The use of a lower alginate content in the 80:20 wt% formulation although increased its injectability and viscosity, it however contributed to a structurally weak and instable end product upon setting. Washout becomes a major problem to bone filler when it is exposed to biological liquids as it may fail to set and form a robust structure to support the bone defect at the application site (Lin et al., 2010). Based on the results of the study, nCSP-Alg bone filler with 70:30 wt.% composition was found to exhibit the best properties in regard to injectability, viscosity and anti-washout ability and was thus chosen for further analysis.

Physiochemical analysis plays an important role in formulation of an ideal bone replacement material as chemical composition and morphology are factors possibly involved in influencing the performance of an implant material (Anil et al., 2020). In this study, both XRD and FTIR analysis showed that the addition of sodium alginate as a polymer did not alter or influence the aragonite phase of nCSP during the synthesis reaction. In addition, there was no change in the XRD pattern of the 70:30 wt.% formulation which indicates that the composition used to formulate the bone filler has maintained the crystalline nature of its aragonite phase in the nCSP sample. The results of this study and the results of the previous study using cockle shell powder in the formulation of bone substitute material showed the presence of aragonite form of calcium carbonate as the only mineral phase present without other impurities after the formulation (Mahmood et al., 2017). The purity of the aragonite phase of $CaCO_3$ which exists in the nCSP-Alg bone filler after the fabrication process plays an important role in the apatite formation on the filler surface and the subsequent mineralization process.

Morphological observation of the 70:30 wt.% bone filler upon setting under the scanning electron micrograph showed presence of a highly porous structure that was primarily attributed by the formation of the egg box model structures typically observed with the cross linking of alginate monomers. These pores contribute to the swelling effects of the formulated bone filler facilitating the migration and proliferation of osteoblasts and mesenchymal cells as well vascularization that can accelerate bone regeneration at the application site (Peter et al., 2010). The presence of rod-like nCSP crystallites deposition as shown by the arrows in Figure 5(c) further contributes to the rough surface morphology observed from the micrograph image. According to preliminary studies, rod-like nanoparticles show better interactions with proteins and cells to enhance cellular uptake and intracellular sorting (Barua & Mitragotri, 2013; Zare et al., 2012). Increased surface roughness not only enhances surface area but also allows the binding of more beneficial bioactive molecules for further applications (Yang et al., 2016).

The ability to form apatite layers on the surface of a bone filler material plays a vital role in increasing cellular reactions that could eventually speed up the formation of bone tissue. Besides, the ability to bind with living tissues through the formation of hydroxyapatite layer in vitro and in vivo, has become one of the important features of tissue engineered bioactive material (Chen et al., 2013). This apatite layer can be produced in vitro by soaking the filler material in SBF solution that has an ionic concentration similar to that of human blood plasma.

The quantitative analysis of apatite layers formation in this study after immersion in SBF for 24 hours was determined by SEM observation. SEM micrograph (Figure 6b) showed surface morphological changes and surface crystalline precipitations indicative of presence of inherent bioactivities. Surface observation also noted cauliflower-like apatite globules with needle-like crystal layers that showed the presence of mineralization properties. A previous study by Chen, also reported similar findings when marine corals and nano pearl powder was immersed in SBF (Chen et al., 2013). The presence of polymer fiber network (Figure 6c) depicts the ability of the fabricated bone filler to mineralize when in contact with human body fluid. This thus demonstrated the properties of mineralization of the fabricated composition which acts as a major factor that can enhance cellular reactions by stimulating osteoblast cell activity, thereby supporting the osteoconductive nature of the material.

To further support this, morphological observation on pattern of osteoblast adherence and proliferation on the surface of the bone filler as observed through SEM micrographs at days 3, 7 and 14 indicated an excellent adherence, proliferation and growth of osteoblast on the filler material. Similar morphological changes were previously reported by Sharma et al., (2016) for nano biocomposite scaffolds fabricated using chitosan-gelatin-alginate. Presences of filopodia and lamellipodia observed as projections from the osteoblast is an affirmative indicator of an excellent adherence and proliferation on the bone filler matrices. Formation of calcium nodules apparent after day 7 further points to the start of surface matrix mineralization that enveloped the entire surface of the filler material contributing to a cross fibrillar pattern observed at day 14. Formation of these fibrillar pattern on matrix surfaces is indicative of osteoblasts ability to regulate the mineralization process (Ansari et al., 2021) thus further supporting the osteoconductive nature of the formulated filler material.

CONCLUSION

The results showed the potential use of nCSP-Alg bone filler with 70:30 wt.% composition as a bone substitute material that can be expanded for clinical use. From the characterization study, nCSP-Alg bone filler with 70:30 wt.% composition showed appropriate properties of injectability, viscosity and anti-washout ability for application as a bone substitute material. The fabricated bone filler retained its chemical compositions and provided sufficient morphological characteristics that was able to support the growth, proliferation and subsequent mineralization of the bone filler by osteoblasts indicative of an excellent osteoconductive material. The formulated nCSP-Alg bone filler also emphasizes the potential use of biomaterials such as cockle shells as an alternative source in the fabrication of cost-effective bone fillers that can be manipulated to form bone substitute materials in the field of bone tissue engineering.

AUTHOR CONTRIBUTIONS

The following study was undertaken by Penny George as part of a research project under the supervision of B. Hemabarathy Bharatham for bone filler design and fabrication. Md Zuki Abu Bakar supervised and contributed to the nano cockle shell production and physiochemical characterization while Zariyantey Abdul Hamid supervised and contributed to the undertaking of *in-vitro* studies. The manuscript was written by Penny George and B. Hemabarathy Bharatham who also supervised, edited, and reviewed the content.

ETHICS APPROVAL

Not applicable.

FUNDING

The research is supported by the University Research Grant GUP 2017 021.

CONFLICTS OF INTEREST

The authors declare no conflict of interest in this work.

ACKNOWLEDGEMENTS

The authors would like to acknowledge University Kebangsaan Malaysia for providing the necessary grant, Program of Biomedical Sciences, Faculty of Health Science and Electron Microscopy Unit of UKM for all necessary research facilities provided. The authors also thank Universiti Putra Malaysia for providing the raw materials for

the development of the bone fillers.

REFERENCES

Anil A, Sadasivan A, Koshi E. Physicochemical Characterization of Five Different Bone Graft Substitutes Used in Periodontal Regeneration: An *In Vitro* Study. J Int Soc Prev Community Dent. 2020 Sep 28;10(5):634-642. https://doi.org/10.4103/jispcd.JISPCD_263_20

Ansari S, de Wildt BWM, Vis MAM, de Korte CE, Ito K, Hofmann S, Yuana Y. Matrix Vesicles: Role in Bone Mineralization and Potential Use as Therapeutics. Pharmaceuticals (Basel). 2021 Mar 24;14(4):289. https://doi.org/10.3390/ph14040289

Barua, S., & Mitragotri, S. (2013). Synergistic targeting of cell membrane, cytoplasm, and nucleus of cancer cells using rod-shaped nanoparticles. ACS nano, 7(11), 9558-9570. https://doi.org/10.1021/nn403913k

Bharatham, H., Zakaria, M. Z. A. B., Perimal, E. K., Yusof, L. M., & Hamid, M. (2014). Mineral and physiochemical evaluation of Cockle shell (Anadara granosa) and other selected Molluscan shell as potential biomaterials. *Sains Malaysiana*, *43*(7), 1023-1029.

Bohner, M., & Baroud, G. (2005). Injectability of calcium phosphate pastes. *Biomaterials*, *26*(13), 1553-1563. DOI: https://doi.org/10.1016/j.biomaterials.2004.05.010

Burguera, E. F., Xu, H. H., & Weir, M. D. (2006). Injectable and rapid-setting calcium phosphate bone cement with dicalcium phosphate dihydrate. *Journal of Biomedical Materials Research Part B: Applied Biomaterials: An Official Journal of The Society for Biomaterials, The Japanese Society for Biomaterials, and The Australian Society for Biomaterials and the Korean Society for Biomaterials*, *77*(1), 126-134. https://doi.org/10.1002/jbm.b.30403

Carey, L. E., Xu, H. H., Simon Jr, C. G., Takagi, S., & Chow, L. C. (2005). Premixed rapid-setting calcium phosphate composites for bone repair. *Biomaterials*, *26*(24), 5002-5014. https://doi.org/10.1016/j.biomaterials.2005.01.015

Fukui, Y., & Fujimoto, K. (2012). Bio-inspired nanoreactor based on a miniemulsion system to create organic–inorganic hybrid nanoparticles and nanofilms. *Journal of Materials Chemistry*, *22*(8), 3493-3499. https://doi.org/10.1039/C2JM14661D

Jian-Chih Chen, Jung-Chang Kung, Chih-Hsin Hsieh, Mei-Ju Hou, Chi-Jen Shih, Chun-Cheng Hung, "Mineralization and Osteoblast Cells Response of Nanograde Pearl Powders", *Journal of Nanomaterials*, vol. 2013, Article ID 752863, 7 pages, 2013. https://doi.org/10.1155/2013/752863

Lin, Q., Lan, X., Li, Y., Yu, Y., Ni, Y., Lu, C., & Xu, Z. (2010). Anti-washout carboxymethyl chitosan modified tricalcium silicate bone cement: preparation, mechanical properties and in vitro bioactivity. *Journal of Materials Science: Materials in Medicine*, *21*, 3065-3076. https://doi.org/10.1007/s10856-010-4160-z

Mahmood, S. K., Zakaria, M. Z. A. B., Razak, I. S. B. A., Yusof, L. M., Jaji, A. Z., Tijani, I., & Hammadi, N. I. (2017). Preparation and characterization of cockle shell aragonite nanocomposite porous 3D scaffolds for bone repair. *Biochemistry and biophysics reports*, *10*, 237-251. https://doi.org/10.1016/j.bbrep.2017.04.008

Maulida, H. N., Hikmawati, D., & Budiatin, A. S. (2015). Injectable bone substitute paste based on hydroxyapatite, gelatin and streptomycin for spinal tuberculosis. *Journal of Spine*, *4*, 82-89. https://doi.org/10.4172/2165-7939.1000266

Mohamed, M., Rashidi, N. A., Yusup, S., Teong, L. K., Rashid, U., & Ali, R. M. (2012). Effects of experimental variables on conversion of cockle shell to calcium oxide using thermal gravimetric analysis. *Journal of Cleaner Production*, *37*, 394-3

Ortiz, M., Escobar-Garcia, D. M., Álvarez-Pérez, M. A., Pozos-Guillén, A., Grandfils, C., & Flores, H. (2017). Evaluation of the osteoblast behavior to PGA textile functionalized with RGD as a scaffold for bone regeneration. *Journal of Nanomaterials*, *2017*. https://doi.org/10.1155/2017/4852190

Peter, M., Binulal, N. S., Soumya, S., Nair, S. V., Furuike, T., Tamura, H., & Jayakumar, R. (2010). Nanocomposite scaffolds of bioactive glass ceramic nanoparticles disseminated chitosan matrix for tissue engineering applications. *Carbohydrate Polymers*, *79*(2), 284-289. https://doi.org/10.1016/j.carbpol.2009.08.001

Sato, T., Kikuchi, M., & Aizawa, M. (2017). Preparation of hydroxyapatite/collagen injectable bone paste with an anti-washout property utilizing sodium alginate. Part 1: influences of excess supplementation of calcium compounds. *Journal of Materials Science: Materials in Medicine*, *28*, 1-7. https://doi.org/10.1007/s10856-017-5853-3

Sharma, C., Dinda, A. K., Potdar, P. D., Chou, C. F. & Mishra, N. C. 2016. Fabrication and characterization of novel nano-biocomposite scaffold of chitosan-gelatin-alginate-hydroxyapatite for bone tissue engineering. *Materials Science and Engineering C* 64(March 2016): 416–427. https://doi.org/10.1016/j.msec.2016.03.060

Sony, S., Suresh Babu, S., Nishad, K. V., Varma, H., & Komath, M. (2015). Development of an injectable bioactive bone filler cement with hydrogen orthophosphate incorporated calcium sulfate. *Journal of Materials Science: Materials in Medicine*, *26*, 1-14. https://doi.org/10.1007/s10856-014-5355-5

Turnbull, G., Clarke, J., Picard, F., Riches, P., Jia, L., Han, F., Li, B., & Shu, W. (2018). 3D bioactive composite scaffolds for bone tissue engineering. *Bioactive materials*, *3*(3), 278-314. https://doi.org/10.1016/j.bioactmat.2017.10.001.

Venkatesan, J., Bhatnagar, I., Manivasagan, P., Kang, K. H., & Kim, S. K. (2015). Alginate composites for bone tissue engineering: A review. *International journal of biological macromolecules*, *72*, 269-281. https://doi.org/10.1016/j.ijbiomac.2014.07.008

Yang, W., Yao, C., Cui, Z., Luo, D., Lee, I. S., Yao, J., ... & Kong, X. (2016). Poly (acrylic acid)-regulated synthesis of rod-like calcium carbonate nanoparticles for inducing the osteogenic differentiation of MC3T3-E1 cells. *International Journal of Molecular Sciences*, *17*(5), 639. https://doi.org/10.3390/ijms17050639

Zare, B., Faramarzi, M. A., Sepehrizadeh, Z., Shakibaie, M., Rezaie, S., & Shahverdi, A. R. (2012). Biosynthesis and recovery of rod-shaped tellurium nanoparticles and their bactericidal activities. *Materials Research Bulletin*, *47*(11), 3719-3725. http://dx.doi.org/10.1016/j.materresbull.2012.06.034

Citation:
George, P., Abdul Hamid, Z., Abu Bakar, M. Z., & Bharatham, B. H. (2024). Nano-cockle shell powder and alginate as novel injectable bone filler: A preliminary formulation and characterization study. *Life Sciences, Medicine and Biomedicine*, *8*(1). https://doi.org/10.28916/lsmb.8.1.2024.138

Life Sciences, Medicine and Biomedicine
ISSN: 2600-7207